A Note on Unsaturated Flow in Two-Dimensional Fracture Networks

H. H. Liu, G.S. Bodvarsson, and S. Finsterle

Earth Sciences Division
Lawrence Berkeley National Laboratory
University of California, Berkeley
California

To be submitted to ***Water Resources Research*** as a technical note

Abstract. Although considerable progress has been made in understanding unsaturated flow processes in a single fracture, our knowledge of unsaturated flow in fracture networks remain incomplete. In this study, we present a numerical investigation of steady flow behavior in two-dimensional fracture networks containing thousands of fractures within a 10 m × 10 m domain. Simulation results indicate that flow paths are generally vertical (as a result of gravity-dominated flow behavior), with subhorizontal fractures providing pathways for communications between vertical flow paths, inducing horizontal spreading of these paths. Although many fractures with small trace lengths do not contribute to the global flow through a fracture network, some of them are still connected to the major flow paths and thus contribute to the overall connectivity of the network. They may also considerably affect the interaction between fractures and the matrix. Based on our simulation results, we hypothesize that average spacing between flow paths in a layered system tends to increase with depth as long as flow is gravity-driven. We also discuss the concept of an influence zone of a capillary barrier to describe seepage from fracture networks to underground openings (drifts). Our simulation results imply that three-dimensional fracture network models are needed for providing a more realistic evaluation of capillary barrier effects.

1. Introduction

Understanding flow and transport in unsaturated fractured rock has been one of the most challenging issues in the area of subsurface hydrology, mainly because of the combination of subsurface heterogeneities and inherent nonlinearities [*Liu et al.*, 1998]. Recently, the need to investigate the feasibility of using the unsaturated zone at Yucca Mountain, Nevada, as a potential site for the geological disposal of high-level nuclear waste has generated intense research interests in understanding and modeling flow and transport in unsaturated fractured rock [e.g., *Bodvarsson and Tsang*, 1999; *Pruess et al*., 1999; *Ho*, 1997]. Flow and transport in unsaturated fractured rock is also a process relevant to other areas, such as environmental contamination in arid and semiarid regions [*Pruess*, 1999].

Recently, considerable progress has been made in understanding unsaturated flow processes within single fractures through laboratory investigations and numerical simulations. *Glass et al.* [1996] demonstrated that the main flow mechanism for a vertical unsaturated fracture is fingering that results from gravitational instability and aperture heterogeneities, a finding further supported by numerical model studies [*Birkholzer and Tsang*, 1997; *Pruess,* 1999]. *Tokunaga and Wan* [1997] showed that film flow could be an important mechanism at low fracture saturations. *Faybishenko* [1999] showed that unsaturated flow in a single fracture (and fracture networks) might be described using the concept of nonlinear dynamics (chaos). In their laboratory experiments, *Su et al*. [1999] demonstrated intermittent flow behavior not considered by classical theory. Observations of water invasion into an initially dry fracture replica indicated that flow paths consisted of broad, water-filled regions, known as “capillary islands,” connected by thin threads of

water, or "rivulets." Even though inflow to the fracture replica was kept constant, intermittent flow persisted in the form of cyclic snapping and re-forming of rivulets [*Su et al.*, 1999]. However, how to incorporate these small-scale mechanisms into field-scale models remains a difficult challenge [*National Research Council*, 2001].

Our understanding of unsaturated flow within a fracture network is incomplete while flow process occurring at this scale is of importance for many field-scale applications. This is mainly because of technical difficulties in experimentally observing details of unsaturated flow processes within a fracture network. In this study, we present a numerical investigation of steady flow behavior in two-dimensional unsaturated fracture networks. Fracture network models have been extensively employed for modeling flow and transport processes in saturated rocks. Reviews of fracture network modeling studies have recently been given by *National Research Council* [1996], among others. The relevant studies under unsaturated conditions are relatively limited in the literature. *Kwicklis and Healy* [1993] reported a numerical simulation of steady water movement in a two-dimensional fracture network in a vertical cross-section consisting of less than ten individual fractures. They found that both pressure and flux are highly variable within the fracture network. *Karasaki et al.* [1994] provided a numerical study of unsaturated flow in a two-dimensional fracture network in a horizontal cross-section and observed strong phase interference. *Therrien and Sudicky* [1996] presented a three-dimensional analysis of unsaturated flow and transport in fractured porous media and concluded that fracture interconnectivity creates erratic hydraulic head patterns and irregularly-shaped contaminant plumes. *Finsterle* [2000] reported an evaluation of the continuum approach in modeling seepage from unsaturated fractured rock into underground openings, which

was performed using a discrete feature model. He concluded that (depending on the objective of the study) reasonable results can be obtained with a calibrated continuum model even for fractured systems in which the underlying flow processes are discrete. He also discussed the differences between his discrete feature model and a fracture network model. Most recently, *Liu and Bodvarsson* [2001] used a fracture network model to develop constitutive relationships for a fracture network.

This study differs from the previous studies based on fracture network models in that we include many more fractures in our fracture network model to more realistically represent unsaturated flow behavior at an actual site. We also consider seepage processes from two-dimensional fracture networks into an underground opening such as a waste-emplacement drift. Seepage into underground openings (drifts) is a major factor affecting the performance of the potential repository in the unsaturated zone of Yucca Mountain, Nevada [*Wang et al.*, 1999; *Birkholzer et al*., 1999]. In this study, special attention is given to unsaturated flow patterns within a fracture network and factors that affect seepage into underground openings.

2. Methods

2.1 Construction of a Fracture Network

There are different ways to computationally construct a fracture network, as reviewed by *Chilès and de Marsily* [1993]. In this study, we constructed simple two-dimensional fracture networks consisting of subvertical and subhorizontal fractures. The procedure used to construct the fracture network includes several steps. First, a group of points were randomly generated using a uniform distribution within a vertical cross section. Second,

for each randomly generated point, a fracture (with the randomly generated point as the middle point) was generated. The lengths of the fractures were randomly determined from five groups of fractures that have different trace lengths, but the same probability of occurrence. Orientations and trace lengths were considered to be independent during the numerical procedure for generating fracture networks. The lengths and orientations are consistent with fracture map data collected from detailed line surveys in tunnels for the highly fractured Topopah Spring welded (TSw) unit in the unsaturated zone of Yucca Mountain [*U.S. Geological Survey*, Unpublished report]. Fractures with trace lengths smaller than 0.23 m were not considered in this study. It is believed that small fractures with trace lengths shorter than this cutoff are unlikely to be hydraulically connected with other fractures and therefore are ignored here. Third, iterations of the above two steps were performed to achieve a desired scanline density (number of fractures per unit length in the horizontal or the vertical direction).

An important geometric parameter for a rough-walled fracture is the average effective fracture aperture. As indicated in *Chilès and de Marsily* [1993], it was found that the thickness of a fracture filled with calcite or another material is strongly positively correlated with its trace length. Given this finding, we followed *Liu and Bodvarsson* [2001] and assumed that the average aperture for a fracture, b, can be related to the corresponding trace length by

$$b = cL^d \qquad (1)$$

where c and d are empirical constants, and L is the trace length (m). Based on air permeability and fracture density data, representative mean and variance values of log(b) for the Topopah Spring welded (TSw) unit of the unsaturated zone of Yucca Mountain

were approximately –4.01 and 0.04, respectively [*CRWMS M&O*, 2000a, 2000b], where the unit of aperture is meters. Using the known mean and variance values for log(b) and trace lengths for the five groups of fractures (Table 1), the parameters c and d were determined (based on Equation (1)) to be 1.008×10^{-4} and 0.317, respectively. Consequently, the average fracture apertures can be estimated from Equation (1) for the five groups of fractures; they are given in Table 1.

2.2 Hydraulic Properties for Individual Fractures

Previous studies have shown that an individual rough-walled fracture can be conceptualized as a two-dimensional porous medium, with constitutive relations represented by the *van Genuchten* [1984] model [e.g., *Pruess and Tsang*, 1990; *Kwicklis and Healey*, 1993]:

$$S_e = [1 + |\alpha P_c|^n]^{-m} \qquad (2a)$$

$$k_r = \sqrt{S_e}[1 - (1 - S_e^{1/m})^m]^2 \qquad (2b)$$

where P_c is the capillary pressure, k_r is the relative permeability, α, n, and m are empirical fitting parameters with $m = 1 - 1/n$, and S_e is the effective saturation given by

$$S_e = \frac{S - S_r}{S_s - S_r} \qquad (2c)$$

In Equation (2c), S is the water saturation, S_r is the residual saturation, and S_s is the satiated saturation. The parameter m is an index of aperture size distribution for an individual fracture and is assumed to be 0.633 in this study. We also assigned S_s and S_r to be 1 and 0.01, respectively, for an individual fracture. The parameter α can be approximately determined as the inverse of the air entry value, which is often used in the

soil science literature [*Wang and Narasimhan,* 1993]. Thus, the α value for an individual fracture can be approximately related to the corresponding average aperture by [*Altman et al.,* 1996]:

$$\alpha = \frac{b}{2\sigma \cos\theta} \tag{3}$$

where σ is the surface tension and θ is the contact angle assumed to be zero in this study. It is also well established that the permeability of a parallel-plate fracture of aperture *b* is given by [*de Marsily*, 1986]:

$$k = \frac{b^2}{12} \tag{4}$$

In this study, we assume Equation (4) to be approximately valid for a rough-walled fracture, when the average aperture is used in the equation. The values for hydraulic parameters, determined based on the approaches mentioned above, are summarized in Table 1. Properties for a fracture intersection is randomly assigned as those of intersected fracture.

2.3 Boundary Conditions and Numerical Simulator

A computationally generated fracture network is shown in Figure 1. It has about 2,000 fractures. Intersections of fractures and an underground opening (drift) with a diameter of 5 m are also shown in the figure (solid circles). The entire (or partial) top boundary of the network is connected to a single source that was assigned a flow rate corresponding to an infiltration flux of 5 mm/yr. The latter is the estimated average net infiltration rate for the unsaturated zone at Yucca Mountain [*Flint et al*., 1997]. A free drainage condition is applied at the bottom of the network, and side boundaries are considered impermeable.

The drift itself is set at a reference pressure of 1 bar without a capillary suction (i.e., it is assumed that the air directly adjacent to the drift wall is at 100% relative humidity). Because the focus of this study is on liquid water flow in unsaturated fractures, the matrix is treated as impermeable. A similar treatment was used in previous studies [*Liu and Bodvarsson,* 2001; *Kwicklis and Healy,* 1993].

The steady-state unsaturated water flow through a fracture network is simulated using the numerical simulator TOUGH2 [*Pruess,* 1991], an integrated finite difference code for simulating multidimensional coupled flow and transport of multiphase, multicomponent fluid mixtures in porous and fractured media. A computational mesh was created for the fracture network shown in Figure 1, which has about 16,000 elements.

3. Results and Discussions

Numerical simulations were performed for two fracture networks with the same statistics for fracture distributions (corresponding to two different realizations). Because similar results were obtained for two networks, we only report results for the fracture network shown in Figure 1.

3.1 Flow Paths and Flow Focusing

Figure 2 shows flow paths within the unsaturated fracture network. These paths were determined by excluding fracture segments that have practically negligible water flux values (less than 0.01% of the total water flux at the top boundary). The flow paths are mainly controlled by connected fractures with large trace lengths. Because unsaturated flow in fractures is gravity-dominated [*Liu et al.,* 1998], flow paths are generally vertical.

The subhorizontal fractures provide pathways for communications between vertical flow paths, inducing horizontal spreading of these paths. Fractures with relatively small trace lengths may also be part of the flow paths mainly near intersections between large fractures. The observation that flow paths are relatively sparse and mainly vertical seems to support the argument of *Liu and Bodvarsson* [2001] that capillarity-driven unsaturated flow paths for porous media at a core (local) scale are more tortuous than gravity-driven paths in unsaturated fracture networks. As a result, they proposed a new relationship between relative permeability and saturation for a fracture network (as a whole) by modifying the tortuosity factor in the *Brooks-Corey* [1964] relationship.

The flow pattern in a fracture network also depends on the top boundary conditions. The flow paths shown in Figure 2 are obtained by imposing uniform capillary pressure at the top of the fracture network (Figure 1). In other words, all the fractures that are part of the connected network and linked to the top boundary are active in conducting water. However, as indicated by *Liu et al.* [1998] and *Pruess* [1999], flow focusing occurs at a fracture network scale. They also suggested that spacing of the flow paths is roughly on the order of meters to tens of meters. Therefore, we cannot expect that a uniform capillary pressure condition exists in fractures near a drift in the deep unsaturated zone of Yucca Mountain or other unsaturated sites. Instead, applying a nonuniform capillary pressure distribution at the top boundary seems more realistic. To take this into account, we only allowed fractures in Figure 1 that are connected to the top and located between 0 -1.5 m and 8.5-10 m in the horizontal direction, to be connected to the source element. The spacing between flow paths at the top boundary is generally consistent with the previous discussions regarding unsaturated flow behavior at Yucca Mountain [*Liu et al.,*

1998; *Pruess,*1999]. Total flow rate from the source element to the top of the network remains the same as that used for the simulation shown in Figure 2. The changed boundary condition resulted in two, primarily vertical flow paths, as shown in Figure 3. Neither "communication" between these two flow paths nor significant horizontal spreading occurs. In other words, flow-focusing resulting from the top boundary persists through the network, although the average fracture spacing is much smaller than the spacing between the two flow paths. This finding is also consistent with field observations. For example, *Wang et al.* [1999] reported that an isolated, nearly wet feature with an average width of 0.3 m was observed in an underground tunnel within the unsaturated zone of Yucca Mountain under ambient flow conditions (Figure 4c of *Wang et al*., [1999]). In principle, the existence of the observed flow feature supports the simulated flow pattern shown in Figure 2.

Simulation results shown in Figure 3 may suggest a mechanism of persistence of flow-focusing in fracture networks for layered geological media. For simplicity, let us consider a geological medium that consists of three layers involving a downward unsaturated flow process. We assume that the top layer and bottom layer have 10 (connected) vertical fractures, respectively, and the middle layer has two. Let us further assume that all the vertical fractures are active in the top layer. In other words, the top layer has 10 vertical flow paths. However, owing to the limitation of vertical fracture number, at most there are two vertical flow paths in the middle layer. As indicated in simulation results shown in Figure 3, the bottom layer still likely contains the same number of flow paths as that in the middle layer, although it has more fractures (or pathways) than the middle layers. Therefore, the thought experiment suggests that flow

focusing may be depth-dependent in a layered system, as long as the gravity is the dominant driving force for flow. In this conceptual model, the number of flow paths in fractures tends to decrease with depth in a layered system in which unsaturated flow in the matrix can be ignored. For example, the welded part of the unsaturated zone of Yucca Mountain is a layered system of this kind.

Effects of fracture properties on unsaturated flow patterns in the fracture network are investigated next. While observing no significant change in flow patterns when fracture permeabilities are increased by one order of magnitude, we found that the α factor (Equation (3)) has an important impact on the flow pattern. Figure 4 shows simulated flow paths for the fracture network shown in Figure 1, which was obtained using the same boundary conditions and fracture property values as those used for Figure 2, except that fracture α values are increased by one order of magnitude. Gravity thus becomes a more dominant force for unsaturated flow in Figure 4 than in Figure 2. As a result, some paths shown in Figure 2 disappear in Figure 4. For example, the downward flow path from point *d* disappears (compare Figures 2 and 4). This is because along the subhorizontal fracture segment *cd* (Figure 2), water coming from upstream fractures cannot "climb" to point *d* as a result of reduction of capillary pressure gradient.

3.2 The Role of Small Fractures

As previously discussed, most flow paths in an unsaturated fracture network mainly consists of large fractures that have relatively long trace lengths, mainly because long fractures have a greater possibility of being connected to other fractures that actively conduct water. Therefore, it is common to exclude small fractures (that have relatively

short trace lengths) in determining hydraulic properties as inputs into a continuum-approach-based model for simulating unsaturated flow in fractures [e.g., *CRWMS M&O*, 2000 a]. While our current simulation results generally support this treatment (excluding the small fractures), we also need to recognize the role of small fractures in enhancing fracture-matrix interaction.

Figure 5 shows fracture segments with relatively large saturations (larger than 7%), that correspond to the flow pattern in Figure 2. Because fractures have very small initial saturations (0.1%) during our simulations, the relatively large simulated saturations (under steady state condition) are a signature of connection with (or being a part of) major flow paths. A comparison between Figures 2 and 5 indicates that there are many small fractures connected to the backbone (see Zone *A* in Figures 2 and 5), although they do not contribute to the global flow through the fracture network. However, these small fractures, such as those in Zone A (Figure 2), may be important for processes that are sensitive to interface areas between the matrix and the fractures (that are part of or connected to major flow paths). One process of this kind is matrix diffusion, which is an important mechanism for solute transport in unsaturated fracture rock [*Bodvarsson et al.,* 2000].

Recently, *Wu et al.* [2001, unpublished manuscript] developed a new continuum approach to simulating flow and transport in unsaturated fractured rock. They conceptualized the fracture continuum to consist of two kinds of fractures, “large” and “small”. “Large” fractures are responsible for global flow through unsaturated fractures, whereas “small” fractures enhance the fracture-matrix interface area. The observations

from our simulations (Figures 2 and 5) provide direct evidence of their conceptualization of the fracture continuum.

3.3 Seepage into the Drift and Influence Zone of Capillary Barrier

Seepage is a major concern in evaluating the performance of the potential repository in the unsaturated zone at Yucca Mountain, Nevada. Special attention in this study is given to the capillary barrier effects for seepage into a drift in a two-dimensional fracture network

The concept of capillary barrier was initially developed for unsaturated flow in porous media. Under unsaturated conditions, the rate of water dripping into a cavity is expected to be less than the downward percolation rate. If percolating water encounters the cavity, the relatively strong capillary forces in the formation retain the water, preventing it from seeping into the cavity. Water accumulates at the drift ceiling, where the increase in saturation leads to capillary pressures that are locally less negative than in the surrounding rocks, allowing water to be diverted around the drift. If the lateral hydraulic conductivity is insufficient to divert the water, fully saturated conditions are reached locally, and seepage occurs as the capillary barrier fails. More detailed discussions of physical processes related to the capillary barrier effects and reviews of the relevant studies were recently given by *Birkholzer et al.* [1999] and *Finsterle* [2000].

Our simulation results indicate that the drift does not serve as an effective capillary barrier for unsaturated flow in the two-dimensional fracture networks used in this study. For example, Figure 2 shows no significant lateral flow paths just above the ceiling of the drift. Consequently, the relationships between the relevant hydraulic properties on

seepage for porous media were not observed from our simulations. For example, the increase in permeability within a porous medium will reduce the seepage into the drift by enhancing the lateral flow above the ceiling [e.g., *Birkholzer et al.* 1999]. However, our simulation results (not shown here) indicate that increasing fracture permeability by one order of magnitude does not reduce seepage into the drift.

To better describe the capillary barrier effects for fracture networks, we introduce a term "influence zone of capillary barrier." When percolating water reaches the intersection between a subvertical fracture and the drift ceiling, water starts to accumulate above the intersection point. Because of the surface tension between water and air, water cannot directly seep into the drift. When more water accumulates, the height of an effectively "saturated" fracture segment (which has negative capillary pressure) above the intersection increases. Consequently, capillary pressure within the fracture at the intersection point also increases. If the height of the effectively "saturated" segment is larger than the air entry value of the fracture approximately represented by $1/\alpha$ (where α is defined in Equation (3)), the capillary pressure at the intersection becomes zero, and seepage occurs. However, if the fracture is connected to a lateral flow pathway before the saturated segment reaches the air entry value, seepage would not occur and the capillary barrier becomes effective [*Finsterle* 2000]. Therefore, for an effective capillary barrier, the lateral flow around the drift must occur within a zone that has the ceiling as the lower limit and a boundary (with a vertical distance of $1/\alpha$ from the ceiling) as the upper limit. On the other hand, only fractures within this zone can "feel" the existence of the drift. Therefore, we call this zone the influence zone of capillary barrier. Note that for a fracture network, the influence zone is very thin. For example, if we take $\alpha = 6.17 \times 10^{-4}$

(Pa^{-1}) as a representative value (Table 1), the thickness of the zone ($1/\alpha$ in terms of pressure head) is only 0.17 m. Although we include a large number of fractures in our network (Figure 1), it is very hard to generate significant lateral flow paths within such a thin zone. That explains why the capillary barrier fails in our simulations.

Finally, our simulation results do not imply that a drift cannot act as a capillary barrier for real-world three-dimensional fracture networks. Our two-dimensional network may be considered a fracture network that is parallel to the longitudinal direction of a drift in a three-dimensional domain. This may considerably underestimate the fracture connectivity within the influence zone for a general three-dimensional fracture network. For example, fractures that are perpendicular to the longitudinal direction of the drift may provide significant lateral flow paths within the fracture plane itself and other fractures accessible in the third dimension. Neither of these effects is considered in our simulations. Therefore, three-dimensional fracture network models should be used for providing a more realistic evaluation of this effectiveness.

4. Concluding Remarks

Although considerable progress has been made in understanding unsaturated flow processes in a single fracture, our knowledge of unsaturated flow in fracture networks remain incomplete. In this study, we have presented a numerical investigation of steady flow behavior in two-dimensional fracture networks. The following are the major conclusions:

Major flow paths within an unsaturated fracture network are mainly determined by fractures with relatively large trace lengths. Flow paths are generally vertical, with sub-

horizontal fractures providing pathways for communications between vertical flow paths, inducing horizontal spreading of these paths.

Although many fractures with small trace lengths do not contribute to the global flow through a fracture network, some of them are still connected to the major flow paths and may considerably affect the interaction between fractures and the matrix. This mechanism is especially important for processes that are sensitive to this interaction (e.g., matrix diffusion).

Our simulation results suggest that the average spacing between flow paths in a layered system (different layers having different network characteristics) may be depth-dependent. The average spacing likely increases with depth as long as gravity-driven flow is the dominant flow mechanism within unsaturated fracture networks. We hypothesize that this may be the case in the welded units of the unsaturated zone at Yucca Mountain; this hypothesis needs to be confirmed.

We discussed the concept of influence zone of capillary barrier to describe seepage from fracture networks to underground openings (drifts). Our simulation results imply that fracture orientation and connectivity within the influence zone has a significant impact on the effectiveness of the capillary barrier, and three-dimensional fracture network models are needed for providing a more realistic evaluation of the capillary barrier effects in fractured formations.

Acknowledgment. We are indebted to Sumit Mukhopadhyay at Lawrence Berkeley National Laboratory for his critical and careful reviews of a preliminary version of this manuscript. We also appreciate stimulating discussions with Yvonne Tsang and Yushu Wu. This work was supported by the Director, Office of Civilian Radioactive Waste Management, U.S. Department of Energy, through Memorandum Purchase Order EA9013MC5X between Bechtel SAIC Company, LLC and the Ernest Orlando Lawrence Berkeley National Laboratory (Berkeley Lab). The support is provided to Berkeley Lab through the U.S. Department of Energy Contract No. DE-AC03-76SF00098.

References

Altman, S. J., Arnold, B. W., Barnard, R. W., Barr, G. E., Ho, C. K., McKenna, S. A., and Eaton, R. R., Flow calculations for Yucca Mountain groundwater travel time (GWTT-95). *SAND96-0819*. Sandia National Laboratories, Albuquerque, NM., 1996.

Birkholzer, J., and C. F. Tsang, Solute channeling in unsaturated heterogeneous porous media, *Water Resour. Res., 33*(10), 2221-2238, 1997.

Birkholzer, J., G. Li, C.-F. Tsang, and Y. Tsang, Modeling studies and analyses of seepage into drifts at Yucca Mountain, *J. Contam. Hydrol., 38*, 349-384, 1999.

Bodvarsson, G. S., and Y. Tsang, (Guest Editors), 1999. Yucca Mountain Project, *J. Contam. Hydrol.,* 38, 1-146, 1999.

Bodvarsson, G. S., H. H. Liu, R. Ahlers, Y. S. Wu, and E. Sonnenthal, Parameterization and upscaling in modeling flow and transport at Yucca Mountain, in *Conceptual Models of Flow and Transport in Fractured Vadose Zone*, National Academy Press, Washington, D.C., 2000.

Brooks, R. H., and Corey, A.T., Hydraulic properties of porous media, *Hydrol. Pap. No. 3*. Colorado State Univ., Fort Collins, 1964.

Chil\x9as, J.-P., and D., de Marsily, Stochastic modeling of fracture systems and their use in flow and transport modeling, In Bear, J., C. F. Tsang, and G. de Marsily (eds.), *Flow and Contaminant Transport in Fractured Rock*, San Diego, California: Academic Press, 1993.

CRWMS M&O, *Analysis of Hydrologic Properties Data,* Las Vegas, Nevada, 2000a.

CRWMS M&O, *Particle Tracking Model and Abstraction of Transport Processes,* Las Vegas, Nevada, 2000b.

de Marsily, G., *Quantitative Hydrogeology,* Academic Press, San Diego, CA, 1986.

Faybishenko, B., Evidence of chaotic behavior in flow through fractured rocks, and how we might use chaos theory in fractured rock hydrology. *Proceedings of the International Symposium on Dynamics of Fluids in Fractured Rocks in Honor of Paul A. Witherspoon's 80th Birthday. Lawrence Berkeley Laboratory Report LBNL-42718*, Berkeley, CA, 1999.

Finsterle, S., Using the continuum approach to model unsaturated flow in fractured rock, *Water Resour. Res. 36* (8), 2055-2066, 2000.

Flint, A. L., J. A. Hevesi, and L. E. Flint, Conceptual and numerical model of infiltration for the Yucca Mountain Area, Nevada, *U.S. Geol. Surv. Water Resour. Invest. Rep.* 1997.

Glass, R. J., M. J., Nicholl, and V. C., Tidwell, Challenging and improving conceptual models for isothermal flow in unsaturated, fractured rocks through exploration of small-scale processes, Rep. *SAND95-1824*, Sandia National Laboratories, Albuquerque, NM, 1996.

Ho, C. K., Models of fracture-matrix interactions during multiphase heat and mass flow in unsaturated fractured porous media, Sixth symposium on multiphase transport in porous media, *ASME International Mechanical Engineering Congress and Exposition*, Dallas, TX, 1997.

Karasaki, K., S., Segan, K., Pruess, and S., Vomvoris, A study of two-phase flow in fracture networks, in *Proceedings of the Fifth Annual International High-Level Radioactive Waste Management Conference,* Am. Nucl. Soc., La Grange, IL, 1993.

Kwicklis, E. M. and Healey, R. W., Numerical investigation of steady liquid water flow in a variably saturated fracture network, *Water Resour. Res., 29* (12), 4091–4102, 1993.

Liu, H. H., C. Doughty and G. S. Bodvarsson, An active fracture model for unsaturated flow and transport in fractured rocks, *Water Resour. Res., 34* (10), 2633–2646, 1998.

Liu, H.H. and G.S. Bodvarsson, Constitutive relations for unsaturated flow in fracture networks, *J. of Hydrology* (in press), 2001.

National Research Council, *Rock Fractures and Fluid Flow, Contemporary Understanding and Applications,* National Academy Press, Washington, D.C., 1996.

National Research Council, *Conceptual models of flow and transport in the fractured vadose zone,* National Academy Press, Washington, D.C., 2001.

Pruess, K., A mechanistic model for water seepage through thick unsaturated zones in fractured rocks of low matrix permeability, *Water Resour. Res., 35* (4), 1039-1051, 1999.

Pruess, K. and Tsang, Y.W., On two-phase relative permeability and capillary pressure of rough-walled rock fractures, *Water Resour. Res., 26*(9), 1915-1926, 1990.

Pruess, K., TOUGH2-A general purpose numerical simulator for multiphase fluid and heat flow, *Rep. LBNL-29400*, Lawrence Berkeley National Laboratory, Berkeley, CA, 1991.

Su, G.W., J.T. Geller, K. Pruess, and F. Wen, Experimental studies of water seepage and intermittent flow in unsaturated rough-walled fractures. *Water Resour. Res., 35* (4), 1019-1037, 1999.

Therrien, R., and E.A. Sudicky, Three-dimensional analysis of variably-saturated flow and solute transport in discretely-fractured porous media. *J. Contam. Hydrol., 23*, 1-44, 1996.

Tokunaga, T. K., and J. Wan, Water film flow along fracture surface of porous rock, *Water Resour. Res. 33*(6), 1287-1295, 1997.

van Genuchten, M. Th., A closed form equation for predicting the hydraulic conductivity of unsaturated soils. *Soil Sci. Soc. Am. J., 44*, 892-898, 1980.

Wang, J.S. Y., R.C. Trautz, P.J. Cook, S. Finsterle, A.L. James, and J. Birkhozer, Field tests and model analyses of seepage into drift, *J. Contam. Hydrol., 38*, 323-347, 1999.

Wang, J.S.Y. and Narasimhan, T.N., Unsaturated flow in fractured porous media, In Bear, J., C. F. Tsang, and G. de Marsily (eds.), *Flow and Contaminant Transport in Fractured Rock.* Academic Press, San Diego, California, 1993.

Table 1. Fracture Properties

Fracture Group	Trace Length (m)	Average Aperture (m)	Permeability (m^2)	α (Pa^{-1})	m (-)
1	0.23	6.3E-5	3.33E-10	4.39E-4	0.633
2	0.32	7.0E-5	4.11E-10	4.88E-4	0.633
3	0.67	8.9E-5	6.57E-10	6.17E-4	0.633
4	1.41	1.1E-4	1.05E-9	7.78E-4	0.633
5	2.65	2.0E-4	3.37E-9	1.40E-3	0.633

Figure 1. A fracture network. The solid circles correspond to intersections between fractures and the outline of a drift.

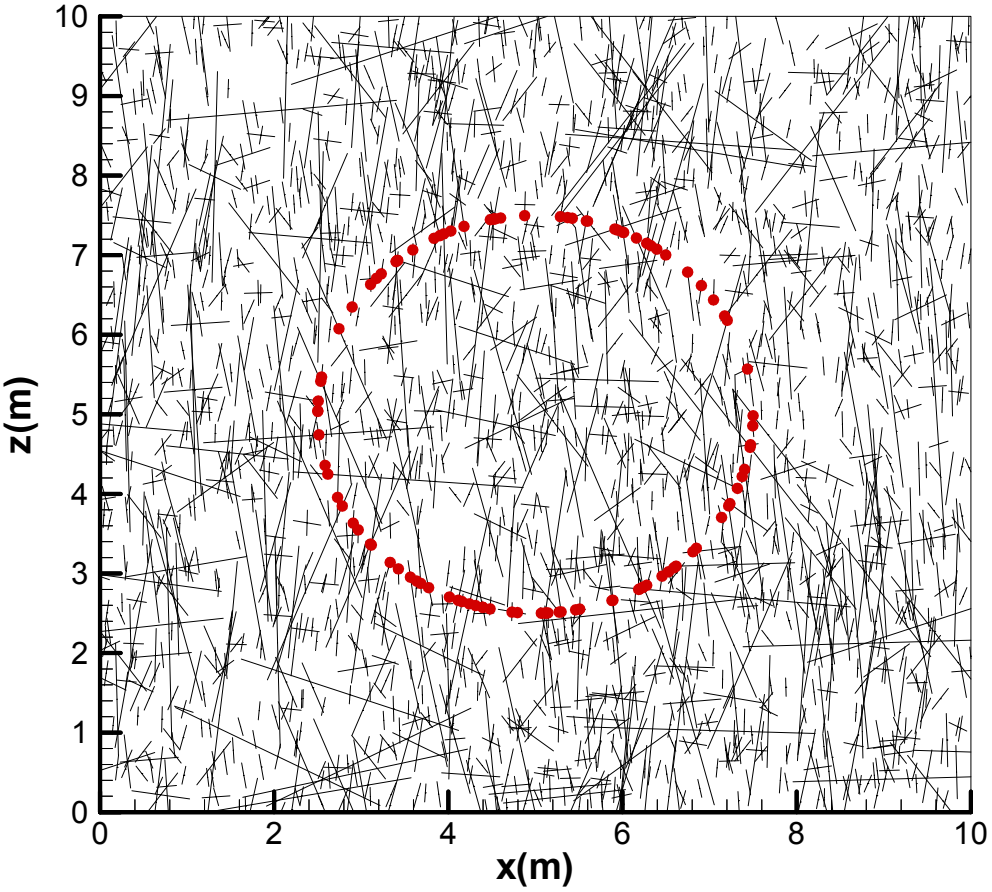

Figure 2. Flow paths in the unsaturated fracture network. The solid circles correspond to intersections between fractures and the outline of a drift.

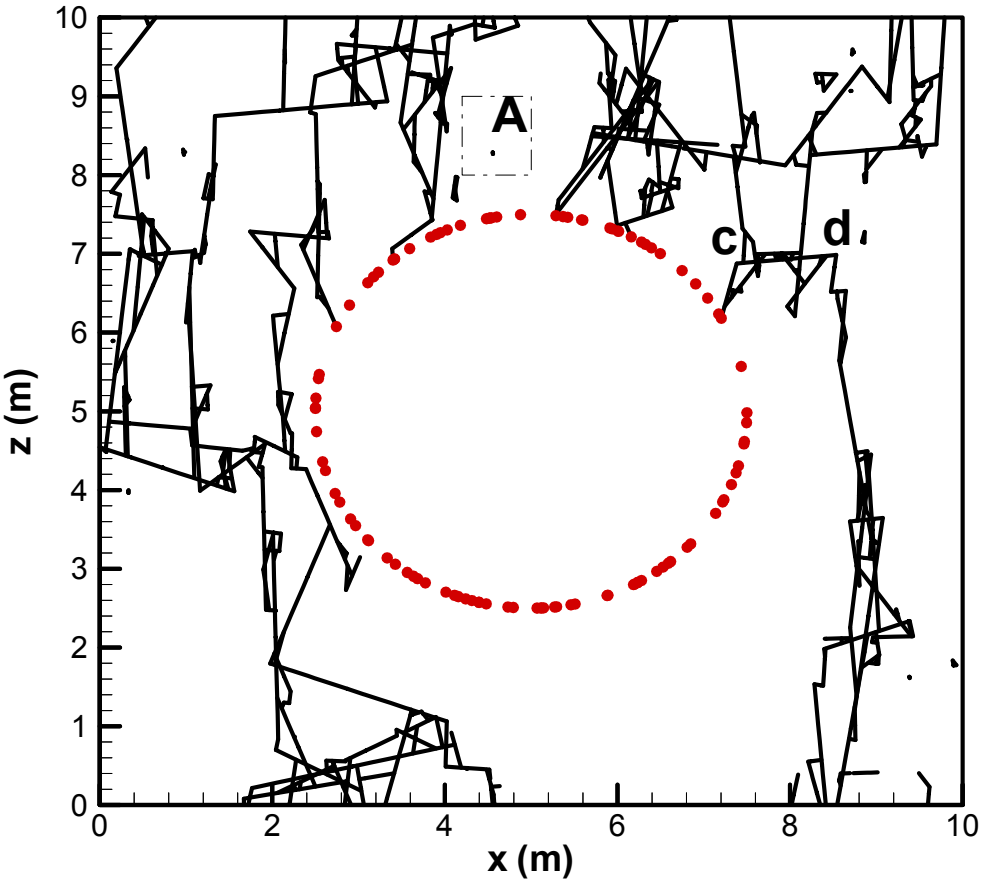

Figure 3. Flow paths when only a portion of fractures at the top boundary (located between 0 to 1.5 m and between 8.5 to 10 m in the x direction) are connected to the source element. The total flow rate from the source element to the fracture network remains the same as that used for Figure 2. The solid circles correspond to intersections between fractures and the outline of a drift.

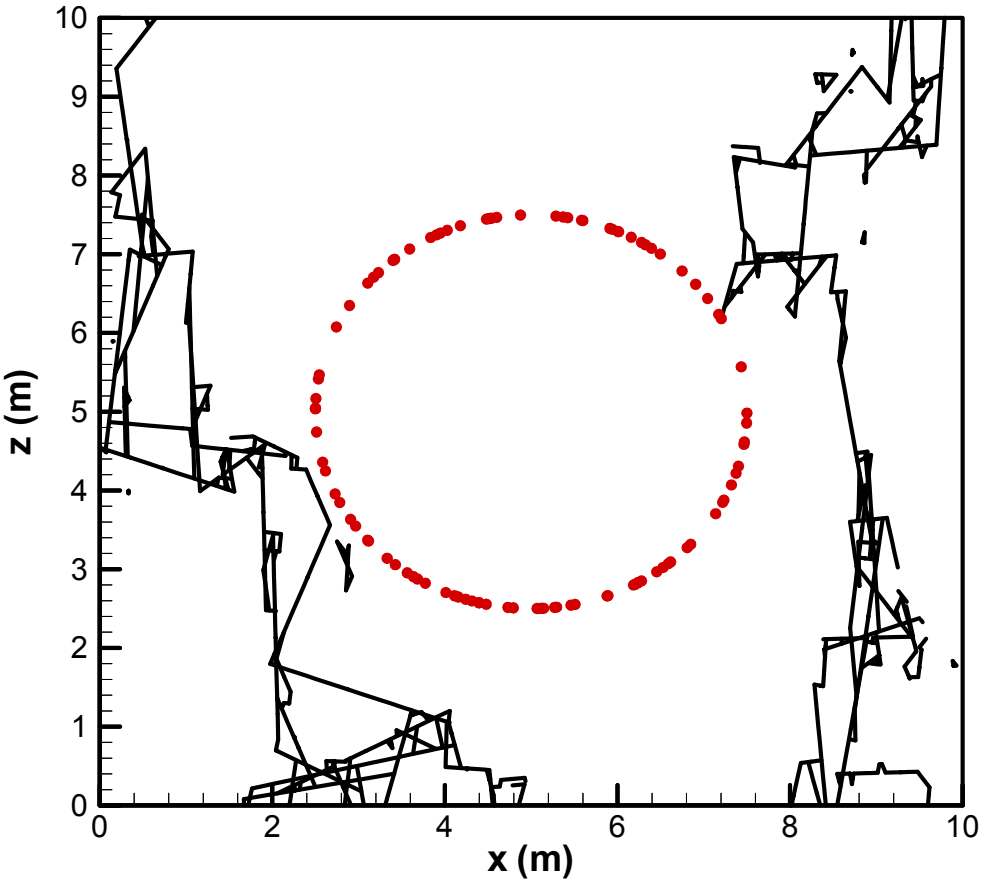

Figure 4. Flow paths for increased α values. The solid circles correspond to intersections between fractures and the outline of a drift.

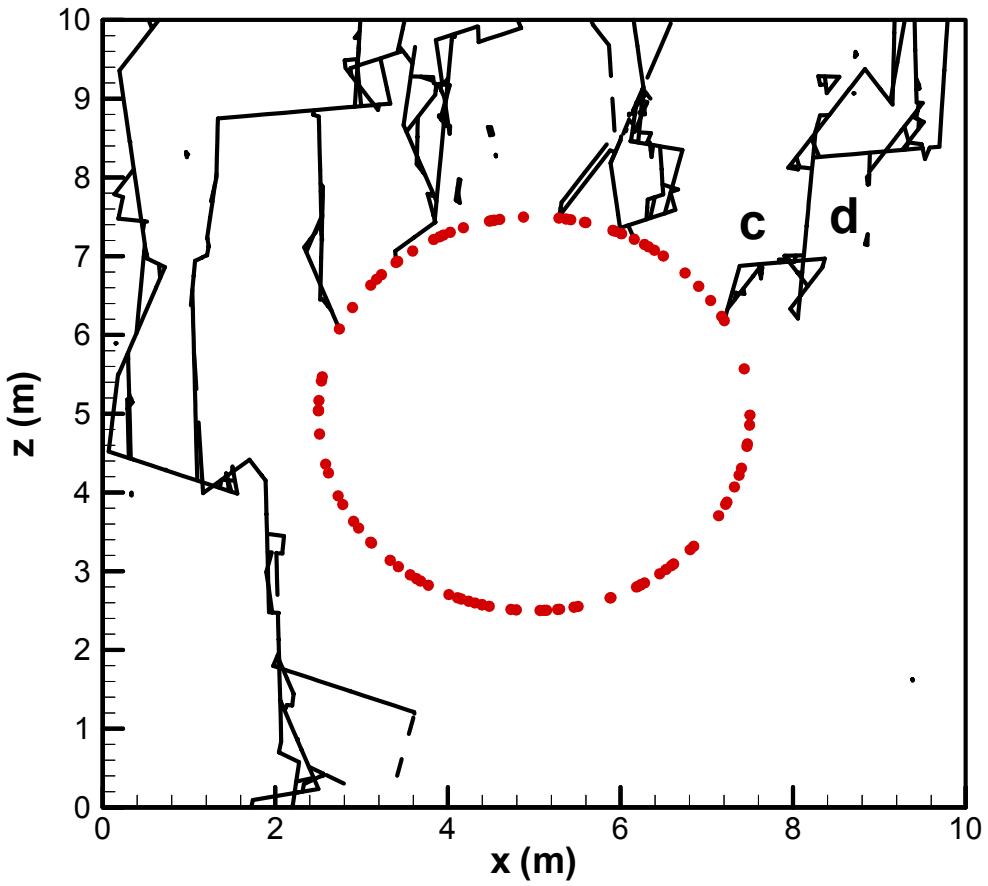

Figure 5. Distribution of fracture segments with saturations larger than 0.07. The solid circles correspond to intersections between fractures and the outline of a drift.